

University of Groningen

## Laser cooling, trapping and spectroscopy of calcium isotopes

Mollema, Albert Kornelis

**IMPORTANT NOTE: You are advised to consult the publisher's version (publisher's PDF) if you wish to cite from it. Please check the document version below.**

*Document Version*

Publisher's PDF, also known as Version of record

*Publication date:*

2008

[Link to publication in University of Groningen/UMCG research database](#)

*Citation for published version (APA):*

Mollema, A. K. (2008). *Laser cooling, trapping and spectroscopy of calcium isotopes*. s.n.

### Copyright

Other than for strictly personal use, it is not permitted to download or to forward/distribute the text or part of it without the consent of the author(s) and/or copyright holder(s), unless the work is under an open content license (like Creative Commons).

The publication may also be distributed here under the terms of Article 25fa of the Dutch Copyright Act, indicated by the "Taverne" license. More information can be found on the University of Groningen website: <https://www.rug.nl/library/open-access/self-archiving-pure/taverne-amendment>.

### Take-down policy

If you believe that this document breaches copyright please contact us providing details, and we will remove access to the work immediately and investigate your claim.

Downloaded from the University of Groningen/UMCG research database (Pure): <http://www.rug.nl/research/portal>. For technical reasons the number of authors shown on this cover page is limited to 10 maximum.

# Chapter 6

## Trap dynamics of even and odd Ca isotopes

### 6.1 Introduction

Magneto-optical trapping [40] of  $^{40}\text{Ca}$  has applications in several fields of research like optical frequency standards [47, 48], Bose-Einstein Condensation (BEC) in alkaline-earth atoms [4, 5], ultra sensitive trace analysis [11, 24, 88] and studies of cold collisions between atoms [49, 89–91]. In each of these applications, a few specific features of the trapped atom cloud are of prime importance. Among these are the density of atoms in the trap, the temperature of the atom cloud and the storage time.

For some experiments, for example to produce metastable calcium atoms [4], just the number of atoms is important and should be maximal. For investigations dealing with cold collisions, the density is a key feature that should be controlled and monitored [89, 90]. The storage time is of importance for spectroscopy and trace analysis applications [11, 48] since longer storage times can improve precision and signal-to-noise ratios in these experiments. The temperature is an other important ingredient. However, remarkably enough, the temperature of a cloud of trapped  $^{40}\text{Ca}$ , like all other even earth-alkaline isotopes trapped in a MOT so far, is higher than the temperature predicted by Doppler theory [16, 40, 43]. For odd isotopes of calcium, like  $^{43}\text{Ca}$  which possess hyperfine structure, one might instead expect a temperature well below the Doppler limit. Temperature measurements performed on an odd isotope of the earth alkaline element Sr,  $^{87}\text{Sr}$  showed a clear sub-Doppler cooling effect [18].

#### 6.1.1 Magneto-optical trapping of $^{40}\text{Ca}$ in literature

In the usual trapping scheme, the strong  $^1S_0 - ^1P_1$  transition at 423 nm is utilized for cooling and trapping of the atoms. When only this transition is used, the average storage time of atoms in a MOT is limited to approximately 20 ms [4, 5, 11, 24, 47, 48, 88],

Ref.	Trapping time (ms)	$I$ (mW/cm <sup>2</sup> )	$\delta$ (MHz)	$T$ (mK)
[47]	20	18	-17	1.6 - 9.5
[48]	20	14	-30	2.2
[4, 5]	22.6		-17	
[24, 88]	18		-120	
[11]	20	12.7		
[49]		9.5	-29	2-3
[89-91]		~200	~84	9

**Table 6.1:** The trapping time, trapping beam intensity ( $I$ ), detuning with respect to the transition frequency ( $\delta$ ) and temperature of a magneto-optically trapped cloud of <sup>40</sup>Ca atoms. In Ref. [47], a temperature of 1.6 mK was measured with a laser intensity of 0.05 mW/cm<sup>2</sup> and 9.5 mK with a laser intensity of 3.6 mW/cm<sup>2</sup>

due to a weak ( $10^{-5}$ ) leak from the  $4^1P_1$  to the  $1D_2$  state, see Figure 2.2.

There are several ways to actually load the trap. In all cases, a metallic sample of calcium is heated in an oven operated at temperatures between 400 and 600 °C. In this way typically atomic beams are created with mean velocities in the order of  $\sim 600$  m/s. It is possible to load the trap directly from such a beam [11, 48]. However, the loading rate of the trap can be enhanced by using the Zeeman slower technique [2], creating an atom beam with a longitudinal velocity on the order of 60 m/s. Kisters et al. [47] and Hoekstra et al. [11] also use a deflection stage to deflect the desired class of atoms out of the Zeeman slowed beam. This has the advantage that the atoms in the MOT are not disturbed by either the atomic beam or the Zeeman slower laser beam passing through the trap chamber. Furthermore, according to Hoekstra et al. a deflection stage is highly isotope selective, and provides the opportunity to trap the different isotopes separately.

For the actual trapping of the atoms, a standard MOT configuration is used. The typical total amount of laser power used by the 6 MOT beams is 10 to 20 mW with a beam diameter on the order of 1 cm. In the experiments described by Kisters et al. [47] and Cavasso Filho et al. [89-91] the beam sizes were considerably smaller, which in the case of Cavasso Filho et al. resulted in rather high intensities up to 200 mW/cm<sup>2</sup>. Typical magnetic field gradients of the MOT are around 40 G/cm. The detuning of the laserlight with respect to the resonance frequency varies between the different experiments. Kisters et al. have reported on a detuning of  $-17$  MHz ( $= \Gamma/2$  with  $\Gamma = 1/2\pi\tau$  where  $\tau$  is the life time of the  $4^1P_1$  state). A similar detuning has been used by Grünert and Hemmerich [4, 5]. Oates et al. use a detuning of  $-30$  MHz and Moore et al. [88] find a maximal trap loading rate at a detuning of  $-120$  MHz. The pressure in the trap chambers used in the experiments varies between  $10^{-9}$  to  $10^{-7}$  mBar.

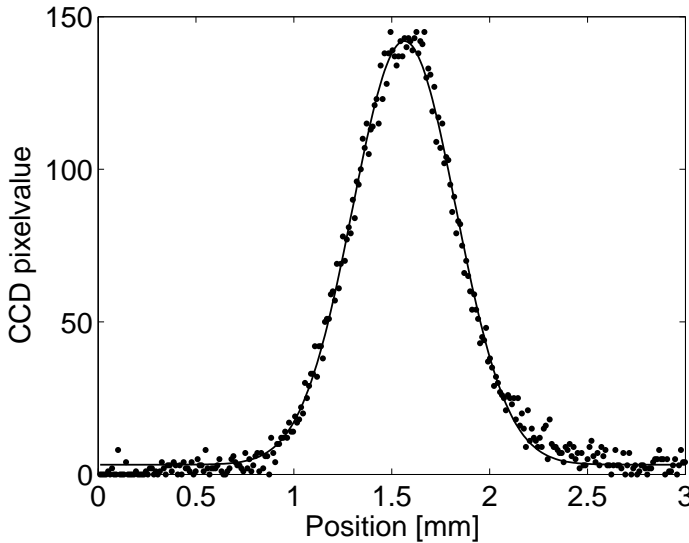
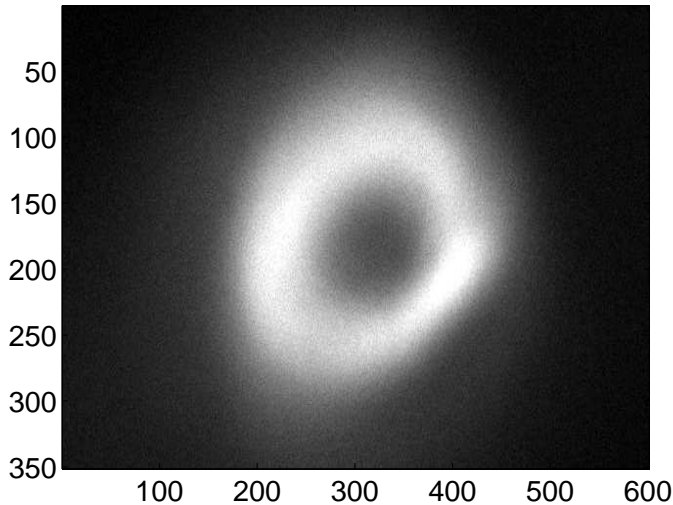


Figure 6.1: Cross section of a CCD image of the MOT. The solid line represents the Gaussian fit.

### Trapping time and repumping

In principle, the average storage time of atoms in a MOT is easily measured. At a certain time the atom flux towards the MOT is terminated, and the fluorescence of the MOT cloud is measured. This fluorescence signal is fitted with a simple exponential decay and the  $1/e$ -time one obtains from such a fit is the trapping time. Table 6.1 summarizes the results from different groups working with Ca MOTs. In all the experiments (except Refs. [89–91] where exceptionally high trapping beam intensities are used) trapping the atoms by using the  $^1S_0 - ^1P_1$  resonance transition only, the average trapping times found are limited to about 20 ms, see Table 6.1. This limit is most likely determined by the electronic structure of Ca (cf. Chapter 2). Due to a weak decay channel from the  $4^1P_1$  to the  $^1D_2$  level, atoms are decaying into the lower lying  $^1D_2$  level at a rate of  $3271 \text{ s}^{-1}$  during the trapping process. About 76 % of these atoms return to the ground state in approximately 3 ms either directly in a quadrupole transition or via the  $4^3P_1$  state which decays via the 657 nm intercombination line. These atoms travel freely during this time. If the illuminated volume of the MOT is sufficiently large (appr. 1 cm in diameter) those atoms will be recaptured and return to the ground state, where they are available again for the trapping transition. The remaining 24 % will decay into the metastable  $^3P_2$  and are lost from the MOT [4, 5, 48]. Some theoretical predictions based on rate equation models for the storage time can be found in refs. [47, 58, 92, 93].

Oates et al. [48] were the first to show that this storage time can be increased by using a so-called repumper. Using a laser at 672 nm, the atoms ending up in the  $^1D_2$



**Figure 6.2:** ‘Doughnut’ or ‘race track’ MOT. On the  $x$  (midplane position) and  $y$  (vertical position) axes the CCD pixel number is indicated. From the calibration a scaling factor of 95.4 pixels/mm was obtained. In this case the vertical laser beams were displaced.

state can be excited to the  $5^1P_1$  state and from there the atoms can decay either back into the  $1D_2$  or  $1S_0$  ground state. After a few cycles, there is a high probability that the atoms finally have decayed back to the ground state again, and thus loss to the  $3P_2$  state has been prevented. A repumper was used in several experiments [4,5,11,24,48,49,88], and the resulting storage times varied between 60 to over 200 ms.

### Temperature

Due to the absence of hyperfine structure effects the even isotopes of alkaline earth elements (which are most abundant), isotopes like  $^{40}\text{Ca}$  and  $^{88}\text{Sr}$  seemed to be ideal testing grounds for Doppler cooling theory, which is based on a pure two level description of the atomic system. However, first temperature measurements of both calcium [47] and strontium [17] show much higher temperatures than the expected Doppler limit  $T_D$  which is 0.831 mK in the case of  $^{40}\text{Ca}$ . The values found experimentally vary between 1.6 and 9.5 mK, see Table 6.1.

In 2003, Xu *et al.* reported on the first single stage sub-Doppler cooling of  $^{87}\text{Sr}$ . In contrary to the even isotopes, the odd isotopes do have a non-zero nuclear spin and therefore possess hyperfine structure, which is a needed ingredient for sub-Doppler cooling in a  $\sigma^+ - \sigma^-$  cooling scheme that can be achieved in a standard MOT [40]. Using the same code that was used by Xu *et al.*, calculations have been done to investigate the possibility of single-stage sub-Doppler cooling in odd isotopes of calcium [94].

First results of this calculation show that sub-Doppler cooling in odd isotopes of calcium seems to be possible, too. Given the fact that it has the highest abundance of the stable odd isotopes of calcium,  $^{43}\text{Ca}$  is a good candidate for testing the prediction that also the odd isotopes of Ca may exhibit sub-Doppler cooling.

## 6.2 General features of our Ca MOT

As described in Chapters 2 and 3, atoms can be trapped in a MOT. When the MOT laser beams are aligned carefully, the density distribution of the MOT will be Gaussian, see Fig. 6.1 where a mid-plane cross section of a CCD image of the MOT cloud is shown. It turns out, however, that trapping atoms in a MOT is the result of a delicate balancing act. For example, when one pair of laser beams is slightly displaced ( $\sim 2$  mm) such that they are not completely overlapping anymore, a MOT configuration shown in Fig. 6.2 can be obtained. Characteristics of such a ‘doughnut’ or ‘race track’ configuration are described in literature (cf. [95, 96] and references therein). Another example showing how easily the MOT configuration can be disturbed is shown in Fig. 6.3, where an on-resonance laser beam (0.8 mm  $1/e^2$  waist) of  $60 \mu\text{W}$  only is sent through the MOT cloud, resulting in a displacement of the cloud of more than one millimeter (about 3 cloud radii).

Typical trap settings for our Ca trap are a detuning  $\delta$  of  $0.5 - 2\Gamma$  and a relative intensity  $s_0 = I/I_0$  of  $0.04 - 0.3$ . The typical magnetic field gradient in the horizontal plane is  $40 - 50$  G/cm. The maximum number of  $^{40}\text{Ca}$  atoms trapped in the MOT is estimated to be in the order of  $10^6$  atoms (see Chapter 3). The limiting factor in this case seems to be the flux of atoms towards the MOT together with atomic structure losses, as discussed in Chapter 2. This relatively low number of trapped atoms results in a low density, where Ca-Ca collision losses are negligible [8].

## 6.3 MOT cloud temperatures of even isotopes

The temperatures of the trapped atoms have been measured using two different techniques: the cloud size method and the release and recapture (RR) method.

### 6.3.1 Cloud size method

As explained in Chapter 2, the temperature of atoms trapped in a MOT can be determined by measuring the radius of the MOT cloud. Apart from the cloud radius, we need to know the spring constant  $\varkappa$ , which in the case of even isotopes can be calculated using Doppler theory ([17], see also Chapter 2):

$$\varkappa = \frac{\mu'}{\hbar k} \beta \frac{\partial B}{\partial x}. \quad (6.1)$$

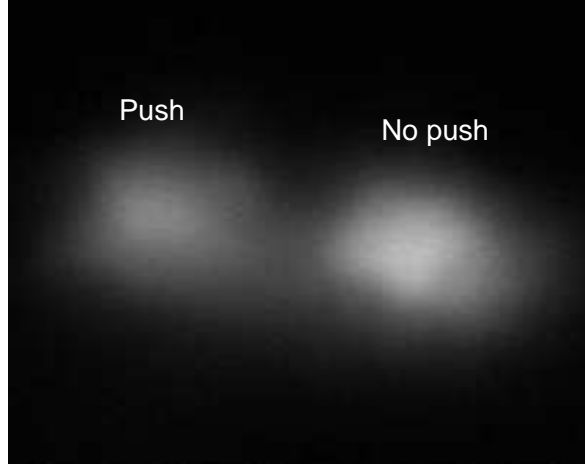


**Figure 6.3:** Displacement of the MOT cloud when a  $60 \mu W$  on-resonance laser beam is sent through the MOT cloud. The picture is the sum of two background subtracted CCD pictures.

The radius is measured using a CCD camera, taking images of the cloud. The CCD data are fitted with a Gaussian line shape:

$$G(x) = b + f \exp \left[ - \left( \frac{x - x_0}{\sqrt{2}\sigma} \right)^2 \right] \quad (6.2)$$

from which the radius is obtained as a fitting parameter ( $\sigma$ ). The temperature  $T$  is now obtained from [17]

$$k_B T = \varkappa \sigma^2 \quad (6.3)$$

### 6.3.2 Release and recapture method

In order to obtain the rms-velocity ( $v_{rms}$ ) of the velocity distribution of the cold atom cloud trapped in the MOT, the MOT-laser light is switched off for an off-time  $t_{off}$ , typically in the order of one to a few ms. When the laser is switched on again, the fluorescence of the trap is measured, and from this data the recaptured fraction can be determined. When this measurement is repeated for several off-times, the recaptured fraction as function of off-time is known, and from this information, together with the capture radius  $r_{capt}$  of the trap the rms-velocity and thus the temperature  $T$  can

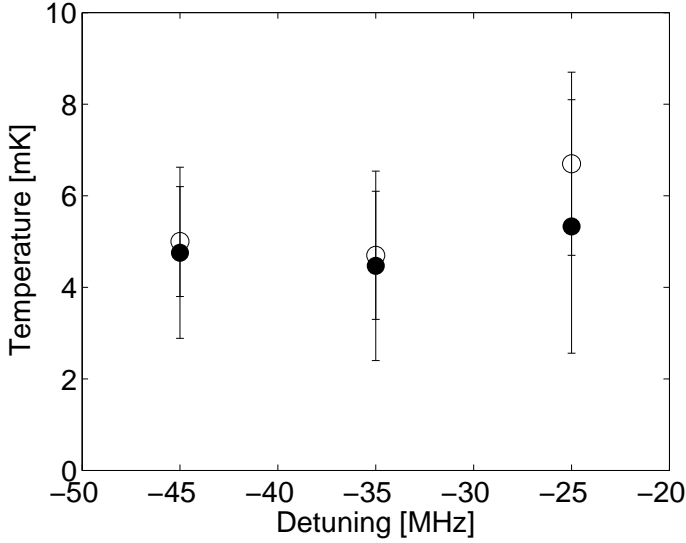


**Figure 6.4:** Comparison between MOT cloud temperatures obtained by the RR and cloud size method: RR data (○), cloud size data (●).

be determined. Assuming an initial Maxwell-Boltzmann velocity distribution and a ballistic expansion after the trapping light is switched off, the fraction  $f$  of atoms that is recaptured immediately after the light is switched on again is given by [6, 97, 98]:

$$f = \operatorname{erf} \left( \sqrt{\frac{m}{2k_B T}} \frac{r_{\text{capt}}}{t_{\text{off}}} \right) - \frac{2}{\sqrt{\pi}} \left( \sqrt{\frac{m}{2k_B T}} \frac{r_{\text{capt}}}{t_{\text{off}}} \right) \exp \left[ -\frac{m}{2k_B T} \left( \frac{r_{\text{capt}}}{t_{\text{off}}} \right)^2 \right] \quad (6.4)$$

where  $m$  is the mass of the atom and  $k_B$  is the Boltzmann constant.

Two methods were applied to switch the MOT laser light. The first approach is adapted from [99]. A mechanical chopper wheel (Scitec Instruments 300C) was extended with a strip of copper foil, such that it chopped the beam with a duty cycle of  $\ll 1\%$ . Off-times of  $\sim 1.5$  up to 10 ms could be achieved this way. Using the second approach, the MOT light was switched by using two acousto-optical modulators (AOM) in sequence, both operated at the same frequency (200 MHz). The  $-1$ st order of the first AOM is coupled into the second AOM of which the  $+1$ st order is used for the MOT. By switching one of the AOMs, which can be done on a time scale of nanoseconds, the light to the MOT is switched. An arbitrary waveform generator produces an on-off signal that switches one of the AOMs and triggers the PCI-based multi-scalar card measuring the countrate of the photon multiplier tube (PMT) that measures the trap fluorescence. In both cases, the recaptured fraction in the trap was determined by



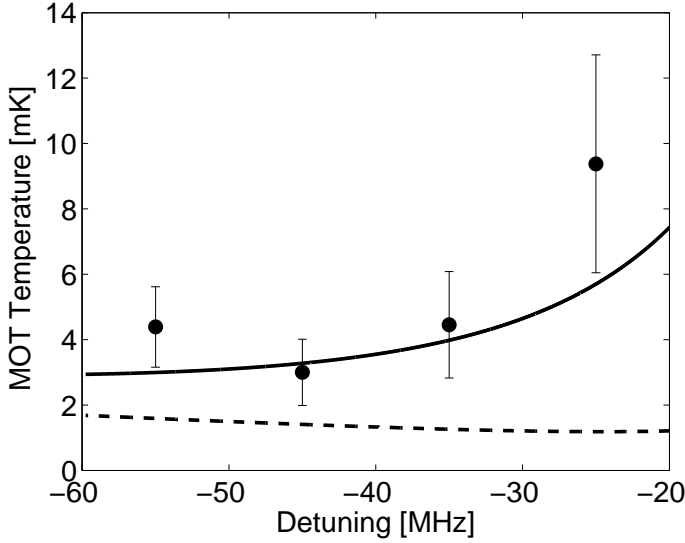


**Figure 6.5:**  $^{42}\text{Ca}$  MOT cloud temperature vs. laser detuning. Dashed line: Doppler theory. Solid line: Choi et al. [51] (see text). The MOT was operated at  $s_0 = 0.17$ .

measuring the trap fluorescence with the PMT. The obtained  $f$  vs.  $t_{\text{off}}$  spectra were fitted with the equation

$$f = \text{erf}\left(\sqrt{\frac{m}{2k_B}} \frac{K}{t_{\text{off}}}\right) - \frac{2}{\sqrt{\pi}} \left(\sqrt{\frac{m}{2k_B}} \frac{K}{t_{\text{off}}}\right) \exp\left[-\frac{m}{2k_B} \left(\frac{K}{t_{\text{off}}}\right)^2\right] \quad (6.5)$$

where  $K = r_{\text{capt}}/\sqrt{T}$ . Since  $r_{\text{capt}}$  and  $T$  are correlated, it is impossible to extract both quantities separately from a fit to the data. Therefore the radius of the MOT beams was taken as  $r_{\text{capt}}$ , giving an upper limit for the fitted  $T$ .

### 6.3.3 Discussion

The comparison of the two available measurement methods to determine the MOT cloud temperatures is presented in Fig. 6.4 and shows good agreement between the RR and cloud size method. For the systematic measurements of  $T$  vs.  $\delta$  and  $s_0$  the cloud size method was used, given the fact that the experimental procedure needed for this method is more convenient. In Fig. 6.5 the MOT temperature as function of the detuning  $\delta$  is shown, Fig. 6.6 shows the data as a function of the saturation parameter  $s_0$ . These experimental results are in agreement with results of  $^{40}\text{Ca}$  temperature measurements that can be found in literature [47–49].

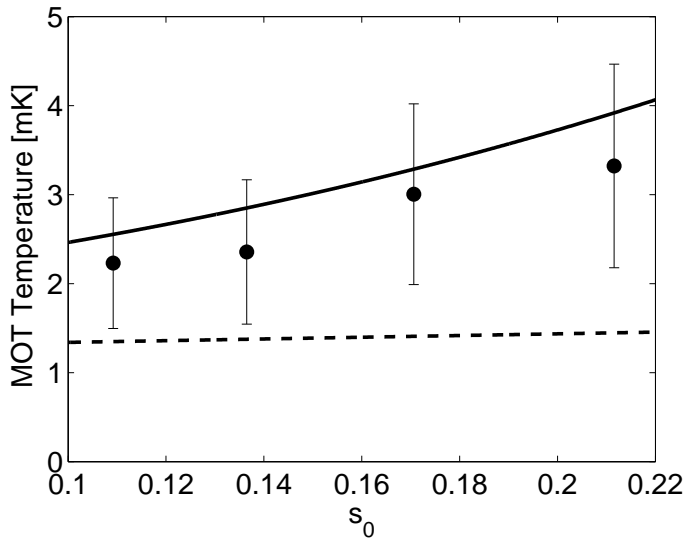


**Figure 6.6:**  $^{42}\text{Ca}$  MOT cloud temperature vs.  $s_0$ . Dashed line: Doppler theory. Solid line: Choi *et al.* [51]. The MOT was operated at  $\delta = -45$  MHz.

Like in any temperature measurement of even alkaline earth elements performed before temperatures well above the Doppler limit are found. The present measurements show temperatures exceeding the Doppler limit by factors of 1.5 – 4 depending on the laser intensity and detuning. Only recently, theoretical work was performed to explain this systematic deviation in detail [50, 51].

### Laser intensity fluctuations

Chanelière *et al.* [50] developed a model in which they took the intensity fluctuation of the trapping laser beams explicitly into account. The intensity fluctuations might induce an extra heating mechanism that could explain the difference between the measured temperatures and the temperatures predicted by Doppler theory. In their model, Chanelière *et al.* define a rms velocity of the atoms  $\sigma_v$  given by

$$\sigma_v^2 = \sigma_D^2 + \sigma_\infty^2 \quad (6.6)$$

where  $\sigma_D$  is the rms velocity as predicted by Doppler theory and  $\sigma_\infty$  is the term describing the additional heating due to fluctuations in the laser intensity

$$\sigma_\infty = \sqrt{2} \frac{\Gamma}{k} \frac{1 + |\Delta|^2 + 2s_0}{4|\Delta|} r_s \quad (6.7)$$

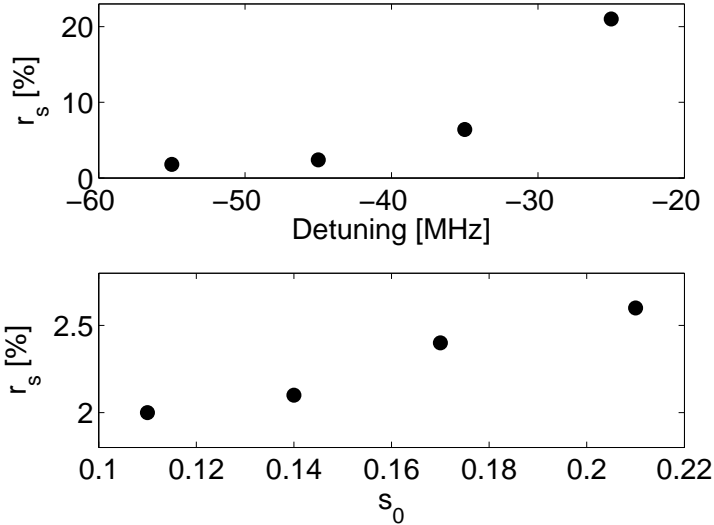


**Figure 6.7:** Average laser intensity fluctuation  $r_s$ , determined from the present data (presented in Figs 6.5 and 6.6) by applying the model by Chaneilère et al. [50]:  $r_s$  vs. detuning (upper panel) and  $r_s$  vs.  $s_0$  (lower panel).

where  $k$  is the norm of the wave vector,  $\Delta = 2\delta/\Gamma$  and  $r_s$  a parameter that represents the average intensity fluctuation in the laser beams with respect to a pure Gaussian intensity profile [50]. This model was designed to explain 1D Doppler cooling, however, the authors claim that the model should also explain 3D cooling like in a MOT, albeit perhaps only qualitatively. In order to check whether the Chaneilère model applies for the present Ca data the model was fitted to the data, resulting in a value for  $r_s$  for every data point. The result of this fitting procedure is given in Fig. 6.7.

When  $s_0$  is varied, see Fig. 6.7 (lower panel), the values of  $r_s$  (average intensity fluctuation) in the order of  $\sim 2 - 2.5\%$  are found, which are not unrealistic numbers. Fig. 6.7 (upper panel) on the other hand shows that an order of magnitude higher  $r_s$  values are needed to explain the measured temperatures while only the detuning is changed from -55 to -25 MHz. It is unlikely that actual fluctuations in laser intensity of 20% do occur.

### Higher order expansion of Doppler theory

A second theoretical approach to describe the elevated temperatures found in alkaline-earth element MOTs was very recently presented by Choi et al. [51]. They extended their previous 1D density-matrix approach of laser (sub-Doppler) cooling [100, 101] to 3D for the specific case of (1+3)-level atoms. Alkaline earth atoms like  $^{40}\text{Ca}$ ,  $^{42}\text{Ca}$  and  $^{88}\text{Sr}$  that have no nuclear spin are such (1+3)-level atoms. The density-matrix formal-

ism is used to describe the dipole interaction of the 3D laser field in the MOT with the (1+3)-level atoms. Therefore multiphoton processes responsible for coherences between the sublevels of the upper state are included.

To calculate the atomic motion a Fokker-Planck equation is solved by applying a series expansion with respect to the saturation parameter  $s_0$ . At the center of the MOT and at near-zero velocity the following third-order expansion for the temperature of (1+3)-level atoms is found for laser powers of  $s_0 < 1$  [51]:

$$T = \frac{\hbar\Gamma}{2k_B} \left( \frac{\Gamma}{|\delta|} + \frac{|\delta|}{\Gamma} \right) \left( 1 + \frac{35s_0}{4(1+\delta^2/\Gamma^2)} + \frac{(377+45\delta^2/\Gamma^2)s_0^2}{8(1+\delta^2/\Gamma^2)^2} + \frac{(14571+475\delta^2/\Gamma^2)s_0^3}{32(1+\delta^2/\Gamma^2)^3} \right) \quad (6.8)$$

By making comparison to the temperature measurements on a  $^{88}\text{Sr}$  MOT cloud by Xu et al. [19], Choi et al showed that when including in the temperature expansion terms up to third power in  $s_0$ , a reasonable to good agreement is obtained between theory and experiment. Since the higher order terms are linked to the coherences between the sublevels of the upper state, this indicates that these coherences are likely to be key to the higher temperatures observed in alkaline-earth MOTs.

This implies that by lowering the laser power multiphoton processes get strongly reduced and the differences between 3D model and standard Doppler-theory should become smaller. This trend is indeed observed in Fig. 6.6 which presents MOT cloud temperatures of  $^{42}\text{Ca}$  as a function of  $s_0$ .

As can be seen from figures 6.5 and 6.6 the 3D (1+3)-level atom model describes our  $^{42}\text{Ca}$  data well both as function of detuning and laser power.

## 6.4 Measurements of temperatures of $^{42}\text{Ca}$ and $^{43}\text{Ca}$

Unlike even isotopes of alkali-earth elements, odd isotopes, such as  $^{87}\text{Sr}$  and  $^{43}\text{Ca}$  have a non-zero nuclear spin, giving rise to hyperfine structure in both the ground and excited states. This difference between even and odd alkali-earth isotopes is of importance for the application of laser cooling and trapping techniques; the hyperfine structure might enable sub-Doppler cooling via the  $(\sigma^+ - \sigma^-)$  sub-Doppler cooling mechanism [45]. This should lead to direct below Doppler temperature, single-stage cooling and trapping of odd alkali-earth isotopes in a MOT. For the case of  $^{87}\text{Sr}$  a sub-Doppler temperature of the trapped atoms was indeed measured [18, 19]. Here, measurements to check whether the sub-Doppler mechanism also works for odd isotopes of Ca are presented.

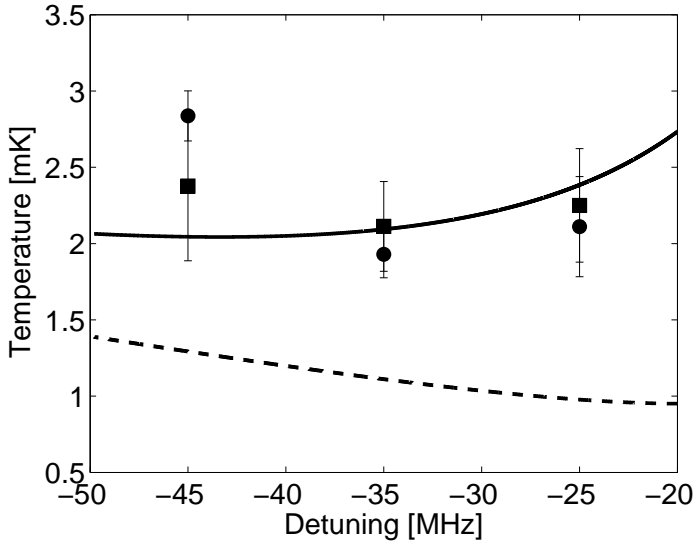


**Figure 6.8:** Results of the release and recapture measurements for both  $^{42}\text{Ca}$  (●) and  $^{43}\text{Ca}$  (■) at different detunings of the MOT laser light. Dashed line: Doppler theory. Solid line: Theory by Choi et al. [51] for  $^{42}\text{Ca}$ . During the measurement  $s_0 = 0.08$ .

### 6.4.1 Experimental setup and results

Given the maximum available laser power for the MOT the saturation parameter  $s_0$  was limited to about 0.1. The temperature of the MOT cloud was measured using the RR technique. The MOT light was switched by using the AOM method. Off-times were varied from 0.5 to 5 ms, and a complete measurement cycle took 500 ms. For each off-time 30 ( $^{42}\text{Ca}$ ) or 90 ( $^{43}\text{Ca}$ ) of these cycles were averaged. More cycles were taken for  $^{43}\text{Ca}$  because of its lower abundance giving rise to a less dense MOT cloud. For both isotopes, data were taken at three different detunings with respect to the cooling transition. Results are given in Fig. 6.8.

### 6.4.2 Discussion

The goal of our experiments was to determine whether there is any significant sub-Doppler cooling effect observable when even and odd isotopes in Ca are trapped under identical conditions. Our measurements reveal that in the conditions present in our Ca MOT there is no significant difference in temperature between  $^{42}\text{Ca}$  and  $^{43}\text{Ca}$  atoms. This outcome is in contrast to the findings for Sr, for which lower temperatures were observed for the odd  $^{87}\text{Sr}$  isotope [18]. Since the data were obtained in a single run of experiments under equal circumstances and the data were treated similarly, possible systematic errors will affect all measurements equally.

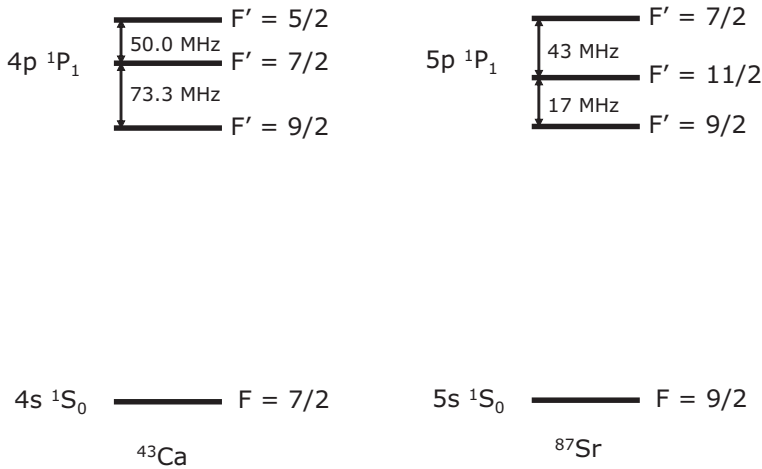


**Figure 6.9:** Hyperfine energy level structure of  $^{43}\text{Ca}$  and  $^{87}\text{Sr}$  relevant to the  $^1S_0 - ^1P_1$  cooling transition. The drawing is not on scale. The  $^1S_0 - ^1P_1$  transition in Sr has a linewidth of 32 MHz.

Although from a laser cooling and trapping point of view there are many similarities between Ca and Sr (for example regarding the natural line width of the cooling transitions, the trap times and reached temperatures), there are differences, especially in the case of odd isotopes, which is illustrated in Fig. 6.9. First of all, the nuclear spin is different for odd Sr and Ca isotopes: 9/2 in the case of  $^{87}\text{Sr}$  and 7/2 in the case of odd Ca isotopes. A  $^{87}\text{Sr}$  MOT operates at the  $^1S_0(F = 9/2) - ^1P_1(F' = 11/2)$  transition while a  $^{43}\text{Ca}$  MOT uses the  $^1S_0(F = 7/2) - ^1P_1(F' = 9/2)$  transition. Moreover, the sequence of hyperfine ( $F'$ ) states and the level spacings of the excited states are different in both cases. For Sr we have (with increasing frequency with respect to the ground state)  $F' = 9/2$ ,  $F' = 11/2$ ,  $F' = 7/2$ , where the level spacing amounts to 17 MHz and 43 MHz respectively [18]. For Ca the  $F'$  states are  $F' = 9/2$ ,  $F' = 7/2$ ,  $F' = 5/2$  where the level spacings are 79 MHz and 42 MHz respectively [20, 39]. Given all these differences, it is not obvious whether or not the sub-Doppler cooling mechanism will work for odd isotopes of Ca.

Together with the temperature measurements on  $^{87}\text{Sr}$ , the authors of [18, 19] also present a model explaining the data. They further evaluate features of the model by artificially increasing the level spacing of the excited state hyperfine manifold by factors of 3, 5 and 1/2, without changing the linewidth (32 MHz) or detuning. When the factor 3 is applied, the sub-Doppler force is significantly reduced. In both other cases, the magnitude of the sub-Doppler force is preserved. These results clearly show that the model description of the sub-Doppler force critically depends on the exact hyperfine structure of the atom at hand, and further more that the model has some striking and uneasily understood features. This model was also applied to  $^{43}\text{Ca}$ , predicting temperatures well below the Doppler temperature [94]. Calculations show an increase in

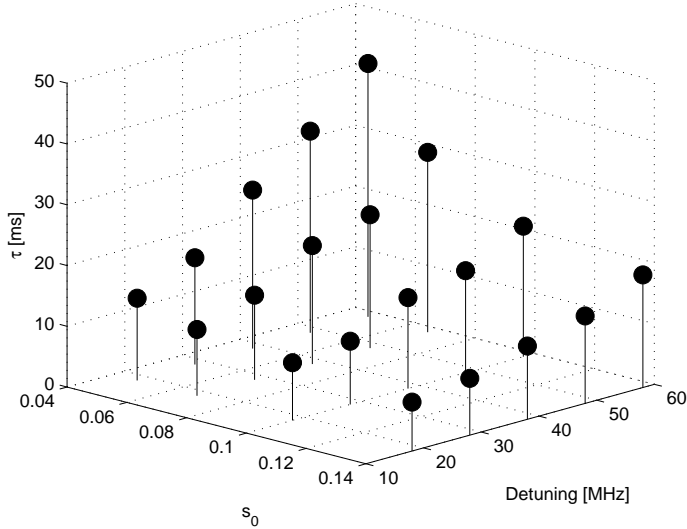


Figure 6.10: Trapping times of  $^{42}\text{Ca}$  for different combinations of laser power and detuning.

sub-Doppler force when the trapping laser intensity is increased. This is in contrast to the experimental findings for  $^{87}\text{Sr}$ , where the temperature of the MOT cloud decreases at decreasing laser power. Further detailed systematic experiments as a function of  $s_0$  and  $\delta$  will be necessary to resolve whether there are no laser settings at all at which sub-Doppler cooling occurs.

## 6.5 Trapping times of atoms in the MOT

### 6.5.1 Experimental method and results

In order to measure the trapping time of the atoms in the MOT, i.e. the time the atoms spend in the trap before they drift out of the trapping region or are lost in the metastable  $^3P_2$  state the flux of the atoms towards the trap needs to be shuttered. This is easily achieved by shuttering the deflection laser beam. For this a home built shutter based on a PC hard disk is used (the design is comparable to that of Maguire et al. [102]). The PMT measures the fluorescence of the trapped atoms. A block signal produced by a signal generator (Krohn Hite model 2000) at  $\sim 1\text{--}2$  Hz triggers both the shutter and the FAST Comtec counter card and after the shutter is closed the fluorescence is measured as a function of time. The data from multiple spectra are averaged and thereafter fitted with an exponential function from which a trapping time  $\tau$  is obtained.

Measurements of trapping times were performed at several MOT parameters, i.e.

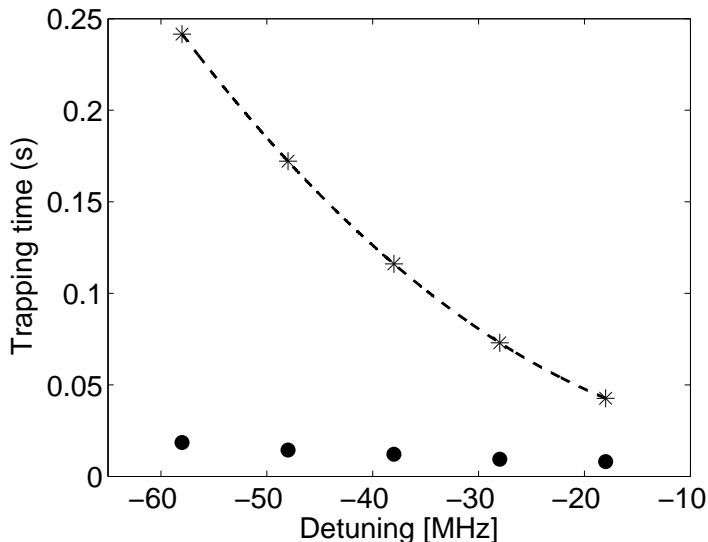


**Figure 6.11:** Comparison between trapping times predicted by the rate equation model (\*) without the drift rate, and the measured data (●) ( $s_0 = 0.14$ ).

at several values for  $\delta$  and  $s_0$ . The obtained data are given in Fig. 6.10 as a 3D stem plot to illustrate the variety of  $\tau$ .

The data can be compared to the results of the rate equation model described in Chapter 2. For the spontaneous transition rates  $\Gamma_{ij}$  the values calculated by Froese Fischer and Tachiev [55] were used. In Fig. 6.11 the data are compared with the predictions from the rate equation model. The extra drift loss rate is not taken into account.

When the drift rate  $R_d = v/d_{tr}$  is included in the model, one can use this rate to fit the model to the data. From the drift loss rate the temperature can be estimated by taking the average velocity. To do so we assumed  $d_{tr}$  to be equal to the diameter of the MOT beams. In Fig. 6.12 the temperature obtained from fitting the rate equation model to the data is compared to temperatures measured in the MOT with comparable trap settings.

### 6.5.2 Discussion

It is obvious from Fig. 6.11 that a rate equation model that only takes into account the transition rates does not explain the observed trapping times in our MOT. Adding the drift rate as an extra loss mechanism and fitting the results of the rate equation model to the data using this rate yields MOT cloud temperatures that are in fair agreement with the temperatures obtained for similar MOT circumstances by the RR and cloud



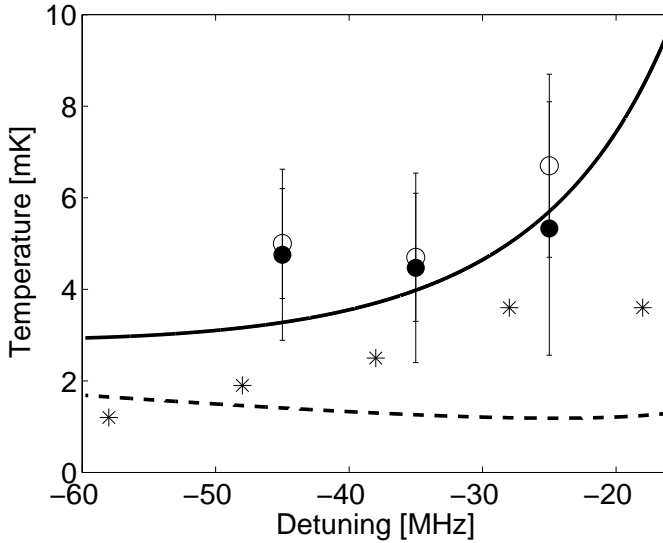


Figure 6.12: Temperature obtained from the rate equation model (\*) and measured using the RR ( $\circ$ ) and cloud size ( $\bullet$ ) techniques. Dashed line: Doppler theory. Solid line: Choi et al. [51].

size method.

## 6.6 Conclusions

The temperature of the MOT cloud of even Ca isotopes was measured using two methods, namely the RR and cloud size method. Results from both methods turn out to be in good agreement with each other. The temperatures found are in good agreement with temperature measurements of  $^{40}\text{Ca}$  by others and are systematically far above the Doppler limit. Two recent models proposed to explain the elevated temperatures of even alkaline earth isotopes in a MOT were tested. The model by Choi et al. [51] was found to be fully consistent with the present data. The comparison with the model by Chanelière et al. [50] was less satisfactory.

The temperatures of even  $^{42}\text{Ca}$  and odd  $^{43}\text{Ca}$  isotopes were measured in identical circumstances using the RR method. No evidence was found for lower temperatures for the odd  $^{43}\text{Ca}$  isotope, which is in contrast with the results obtained from measurements performed on  $^{87}\text{Sr}$  by Xu et al. [18]. The absence of a sub-Doppler cooling mechanism in the case of  $^{43}\text{Ca}$  may be due to the level spacing and ordering of the hyperfine levels of the  $4s4p^1P_1$  state which differ from  $^{87}\text{Sr}$ . It seems that the exact hyperfine structure details of  $^{43}\text{Ca}$  inhibit significant sub-Doppler cooling of  $^{43}\text{Ca}$ .

The trapping times of even Ca isotopes were measured for a large range of trap

---

parameters. The results of the measurements can be understood using a rate equation model when an extra loss mechanism, the temperature dependent drift parameter, is taken into account. Fitting the model to the data using this parameter yields temperatures which given the simplicity of the model are in remarkable good agreement with actual temperature measurements performed for similar trapping conditions.

